



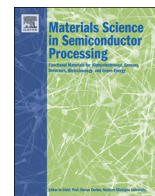
Electrical characterization of high k-dielectrics for 4H-SiC MIS devices

Downloaded from: <https://research.chalmers.se>, 2020-09-20 02:37 UTC

Citation for the original published paper (version of record):

Khosa, R., Chen, J., Winters, M. et al (2019)
Electrical characterization of high k-dielectrics for 4H-SiC MIS devices
Materials Science in Semiconductor Processing, 98: 55-58
<http://dx.doi.org/10.1016/j.mssp.2019.03.025>

N.B. When citing this work, cite the original published paper.



Electrical characterization of high k-dielectrics for 4H-SiC MIS devices

R.Y. Khosa^{a,b,*}, J.T. Chen^c, M. Winters^d, K. Pálsson^a, R. Karhu^c, J. Hassan^c, N. Rorsman^d, E.Ö. Sveinbjörnsson^{a,c}

^a Science Institute, University of Iceland, Iceland

^b Department of Physics, University of Education Lahore, Dera Ghazi Khan Campus, 32200, Dera Ghazi Khan, Pakistan

^c Department of Physics, Chemistry and Biology (IFM), Semiconductor Materials Division, Linköping University, SE-58183, Linköping, Sweden

^d Department of Microtechnology and Nanoscience, Chalmers University of Technology, SE-41296, Göteborg, Sweden

ARTICLE INFO

Keywords:

Interface traps
AlN/4H-SiC interface
Al₂O₃/4H-SiC interface
MIS structure

ABSTRACT

We report promising results regarding the possible use of AlN or Al₂O₃ as a gate dielectric in 4H-SiC MISFETs. The crystalline AlN films are grown by hot wall metal organic chemical vapor deposition (MOCVD) at 1100 °C. The amorphous Al₂O₃ films are grown by repeated deposition and subsequent low temperature (200 °C) oxidation of thin Al layers using a hot plate. Our investigation shows a very low density of interface traps at the AlN/4H-SiC and the Al₂O₃/4H-SiC interface estimated from capacitance-voltage (CV) analysis of MIS capacitors. Current-voltage (IV) analysis shows that the breakdown electric field across the AlN or Al₂O₃ is ~ 3 MV/cm or ~ 5 MV/cm respectively. By depositing an additional SiO₂ layer by plasma enhanced chemical vapor deposition at 300 °C on top of the AlN or Al₂O₃ layers, it is possible to increase the breakdown voltage of the MIS capacitors significantly without having pronounced impact on the quality of the AlN/SiC or Al₂O₃/SiC interfaces.

1. Introduction

The great potential of 4H-SiC MISFETs for power electronics is hampered by low channel mobility mainly due to high density of interface states at the SiO₂/SiC interface. The quality of the SiO₂/SiC interface has been improved by various oxidation and nitridation methods but more reduction in interface traps is needed [1–3]. Beside SiO₂ as a gate dielectric, the use of high-k dielectrics on SiC has also been investigated. AlN and Al₂O₃ have reasonably large band gap (~ 6.2 eV and ~ 7 eV respectively) and high dielectric constant. The conduction band offset of AlN or Al₂O₃ to 4H-SiC of ~ 1.7 eV is expected to be sufficient for n-channel MISFET operation [4–9]. High quality single crystalline AlN can be grown on SiC because of only 1% lattice mismatch to SiC [10]. However, an amorphous Al₂O₃ is considered to be better than poly-crystalline α-Al₂O₃ as a gate dielectric on 4H-SiC because of leakage through grain boundaries [11].

A crystalline AlN grown by molecular beam epitaxy (MBE) has been reported as a gate dielectric for 4H-SiC MISFETs but very low channel mobility (< 1 cm²/V) was obtained because of the leaky structure [12]. The irradiation of atomic nitrogen or HCl gas etching before the growth of AlN has been used to improve the quality of MBE grown AlN films

[13,14]. The growth of AlN layers by MOCVD on 4H- and 6H-SiC has also been reported and a significant density of fixed charge and interface traps is observed in such AlN layers [15,16].

An amorphous Al₂O₃ grown by atomic layer deposition (ALD) or thermal oxidation of metallic Al has been used as a gate dielectric in graphene field effect transistors with some success [17,18]. The ALD as grown Al₂O₃ on 4H-SiC typically contains a large number density of negative charges which are reduced after annealing in Ar at 1000 °C but the Al₂O₃/SiC interface contains a high density of interface traps after such treatment due to growth of an interfacial SiO_x (0 < x < 2) layer [19]. To improve the quality of ALD grown Al₂O₃, pre-deposition surface cleaning and post deposition annealing has been performed in N₂O or N₂ ambient [20,21]. A MOSFET with ALD grown Al₂O₃, that was post-annealed in hydrogen at 400 °C, is reported with a field effect mobility of 57 cm²/V. Even though these results are promising, large threshold voltage shifts are observed due to the sensitivity of the Al₂O₃ layers to electron injection [22]. There is another report on a very high peak field effect mobility of 300 cm²/V in SiC MOSFETs using Al₂O₃ made by MOCVD with a thin SiO₂ interfacial layer to the SiC [23]. But, the mobility drops very rapidly with gate voltage and is less than 50 cm²/V at moderate gate voltages.

* Corresponding author. Science Institute, University of Iceland, Iceland.

E-mail addresses: ryk2@hi.is (R.Y. Khosa), jrche@ifm.liu.se (J.T. Chen), micwinte@chalmers.se (M. Winters), kjp9@hi.is (K. Pálsson), robka36@ifm.liu.se (R. Karhu), jawul@ifm.liu.se (J. Hassan), niklas.rorsman@chalmers.se (N. Rorsman), einars@hi.is (E.Ö. Sveinbjörnsson).

<https://doi.org/10.1016/j.mssp.2019.03.025>

Received 5 September 2018; Received in revised form 7 February 2019; Accepted 20 March 2019

Available online 28 March 2019

1369-8001/ © 2019 The Authors. Published by Elsevier Ltd. This is an open access article under the CC BY-NC-ND license (<http://creativecommons.org/licenses/by-nc-nd/4.0/>).

In this study, we grow crystalline AlN by hot wall MOCVD and amorphous Al₂O₃ by low temperature oxidation of Al on n-type 4H-SiC. On few selected samples, an additional layer of SiO₂ is deposited on top of the AlN or Al₂O₃ layer by plasma enhanced chemical vapor deposition (PECVD). The interface traps at the AlN/SiC and Al₂O₃/SiC interfaces are investigated by capacitance voltage (CV) measurements on MIS capacitors. The dielectric breakdown properties are extracted from current voltage (IV) measurements. We find that both the AlN/SiC and the Al₂O₃/SiC interface contain very low density of interface traps and the use of SiO₂/AlN or SiO₂/Al₂O₃ dielectric stack improves the breakdown voltage of the MIS devices.

2. Experimental methods

Two sets of n-type 4H-SiC MIS capacitors were made. One with single crystalline AlN and other with amorphous Al₂O₃ as a dielectric. The 4H-SiC used in this study have 10 μm thick n-type epitaxial layers with a net doping concentration of $\sim 1 \times 10^{16} \text{ cm}^{-3}$ grown on 4° off-axis (0001) highly doped $\sim 1 \times 10^{18} \text{ cm}^{-3}$ 4H-SiC substrates. A single crystalline 10 nm thick AlN layer was grown on 4H-SiC in a horizontal hot-wall MOCVD reactor at 1100 °C. Ammonia and Al₂(CH₃)₆ were used as a precursor for nitrogen and aluminum respectively. Prior to deposition of AlN, the SiC surface was exposed in H₂ ambient at 1320 °C, in order to obtain a native oxide-free surface. The details of the AlN growth process and structural characterization of the crystalline AlN layers are given in Ref. [24]. The amorphous Al₂O₃ is grown by depositing few monolayers of pure Al by electron beam evaporation at a rate of $\sim 0.5 \text{ \AA/s}$ and then the sample is baked on a hot plate in room environment at a temperature of 200 °C for 5 min to form Al₂O₃ layer. This process of deposition and subsequent low temperature oxidation was repeated twelve times resulting in a film thickness of 15 nm as determined by X-ray reflectivity (XRR) and Atomic Force Microscopy. Prior to growth of Al₂O₃, the SiC was cleaned with HF in order to remove the native oxide. Further details of the Al₂O₃ growth process are given in Ref. [25]. An additional layer of SiO₂ with thickness of 40 nm was deposited on selected samples from both sets by PECVD at 300 °C using source gases of nitrous oxide and silane. Reference MIS capacitors with thermal SiO₂ grown in dry oxygen or in N₂O ambient were also analyzed. Samples with identical reference oxides have previously been used in SiC MOSFETs [26]. The dielectric thickness of all samples was estimated using X-ray reflectivity (XRR) and the crystallinity was investigated with X-ray diffraction (XRD). Our Al₂O₃ and SiO₂ films are amorphous, no crystallization is observed by XRD apart from the AlN samples [24].

Circular MIS capacitors are made using Al as a gate metal and back contact as well. The interface quality is characterized by conventional CV analysis using Agilent E4980A LCR meter. The dielectric breakdown strength of the MIS samples is determined by IV measurements using a Keithley 617 electrometer. CV and IV measurements are performed in vacuum of 10^{-3} mbar in a cryostat.

3. Results and discussion

Fig. 1 shows CV spectra of MIS capacitors having AlN and Al₂O₃ dielectrics measured at room temperature and at frequencies of 1 kHz and 1 MHz. The gate bias is swept from depletion (negative bias) to accumulation (positive bias) and the capacitance signal for both frequencies is recorded simultaneously at each gate bias point. Fig. 1a shows the CV curves for AlN sample. The dielectric constant deduced from the accumulation capacitance is about 8.7. Fig. 1b shows the CV spectra of the Al₂O₃. The dielectric constant for Al₂O₃ is ~ 6.5 . The flatband voltage in both AlN and Al₂O₃ is $\sim 0.7 \text{ V}$ which is close to the theoretical flatband voltage (i.e. $\sim 0.4 \text{ V}$) which shows that initially the AlN and Al₂O₃ layers contain insignificant amount of fixed charge. A first estimate of the interface trap density is extracted from frequency dispersion of CV curves [27]. In the AlN and Al₂O₃ case, such dispersion

is hardly visible indicating a low interface state density.

The interface quality of AlN or Al₂O₃ dielectric with 4H-SiC can be estimated by investigating the frequency dispersion of the CV spectra of an MIS capacitor. Electron capture into interface states is most often a fast process while electron emission from interface traps is normally much slower and is a thermal process which depends on the difference $E_c - E$ (where E is the energy level of the interface trap and E_c denotes the SiC conduction band edge). If an electron is captured and not emitted again, this is detected as a shift of the CV curve to higher gate voltages. If the test frequency is high (1 MHz) then more traps will not emit their electrons and the curve is shifted as compared to the low frequency (1 kHz) curve. The extraction of D_{it} follows the method of Berglund [27]. The interface trap density (D_{it}) is determined by well-known High-Low-Capacitance method using an equation: $D_{it} = \frac{1}{q} \left(\frac{C_d C_{lf}}{C_d - C_{lf}} - \frac{C_d C_{hf}}{C_d - C_{hf}} \right)$. Where C_d is dielectric capacitance, C_{lf} and C_{hf} are low and high frequency capacitance respectively.

Fig. 2 shows D_{it} extracted from room temperature CV dispersion data for MIS samples with AlN or Al₂O₃ as a dielectric as well as reference SiO₂ samples. The single layer AlN and Al₂O₃ samples contain the lowest D_{it} . The detrimental interface states that exist within this energy range for thermally grown oxides are virtually absent at the AlN/SiC or the Al₂O₃/SiC interface. It is clear that the addition of a SiO₂ dielectric layer on the top of AlN or Al₂O₃ affects the AlN/SiC and Al₂O₃/SiC interfaces. However, the single AlN and the SiO₂/AlN stack both have lower D_{it} than reference samples. The D_{it} of the SiO₂/Al₂O₃ stack is comparable to the reference N₂O grown SiO₂.

A sensitivity to electron injection is observed in both AlN and Al₂O₃ samples. This is detected as a flatband shift in subsequent 100 kHz CV curves when the samples are repeatedly biased into accumulation. The magnitude of the shift depends on the maximum applied accumulation voltage. An example of such behavior is shown in Fig. 3 for single layer AlN and Al₂O₃ MIS samples. Such behavior is also reported in literature for AlN and Al₂O₃ MIS samples [14,19]. This flatband shift can be a result of trapping of electrons in defects located within the dielectric. Similar electron injection is also observed in the dielectric stacks (not shown here).

However, in this work the process is reversible since the trapped electrons can be released back to the SiC at room temperature by applying depletion bias stress and UV illumination for a certain time to the MIS capacitors [28–30]. An example of such an experiment is shown in Fig. 4 for AlN/SiO₂ and Al₂O₃/SiO₂ stack samples. In the case of the AlN/SiO₂ sample (Fig. 4a), the MIS capacitor is initially kept in accumulation (+11 V) for 30 min at room temperature and then sequentially the bias with 100 kHz frequency is swept to depletion (−10 V) and the CV is recorded seen as the black solid curve. Electrons are intentionally injected into the AlN layer during the bias stress. Next, a UV light is shined on the sample under depletion bias of −10 V for 30 min to examine if electrons are released from AlN traps. A broken black 100 kHz CV curve is recorded directly thereafter. A stretch-out of the CV curve at gate voltage from −5 V to 7 V suggests that electrons are released from traps during UV exposure, but they are recaptured to traps as the gate voltage leads the device to accumulation. The same procedure is applied to the Al₂O₃/SiO₂ sample with accumulation and depletion bias of +5 V and −5 V respectively (shown in Fig. 4b) and the results are similar to the AlN/SiO₂ sample. This experiment shows that the AlN and Al₂O₃ layers have traps which capture free electrons during accumulation bias stress and re-emission of the captured electrons is made possible by UV illumination. Applying depletion bias in the same manner but without applying UV light results in a negligible shift of the CV curves (not shown).

IV measurements are used to estimate the critical breakdown field of the dielectrics. Fig. 5 compares the dielectric breakdown field of the AlN and Al₂O₃ samples as well as of reference dry SiO₂ sample based on current density measurement as a function of the effective electric field (J-E) across the gate dielectric. A breakdown field of $\sim 3 \text{ MV/cm}$ (solid

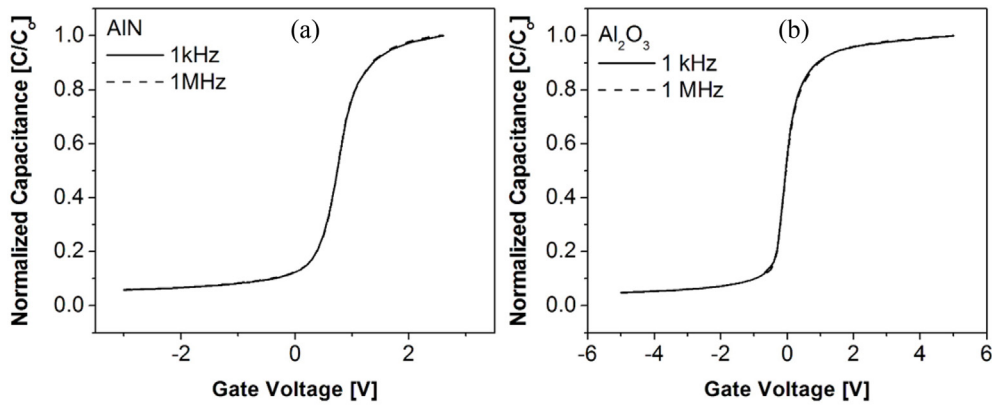


Fig. 1. Room temperature CV curves for (a) AlN and (b) Al₂O₃ samples at test signal frequencies of 1 kHz and 1 MHz.

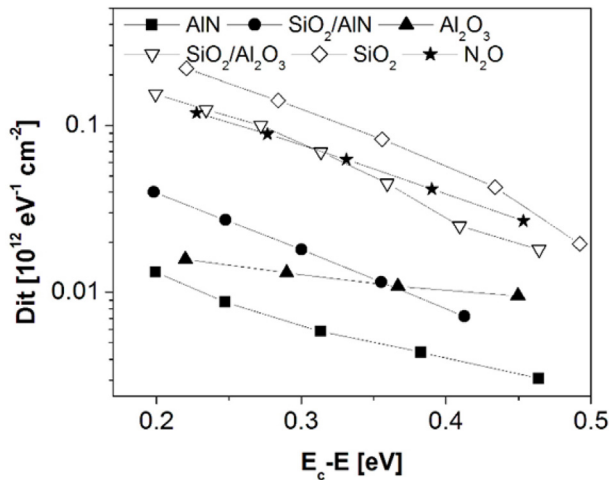


Fig. 2. Comparison of the density of interface states (D_{it}) estimated from CV (at 298 K) as a function of energy for AlN and Al₂O₃ based MIS capacitors along with reference SiO₂ MIS capacitors.

curve) or 5 MV/cm (dotted curve) is recorded for the single layer AlN or Al₂O₃ sample respectively. A sharp current leakage is observed for single layer AlN even at low dielectric electric fields. This suggests the AlN layers have higher density of bulk traps compared to Al₂O₃ that cause trap assisted leakage across dielectric. The breakdown field of the reference thermal SiO₂ sample is ~ 9 MV/cm (dash double dotted curve). The physical origin of the electron traps within the AlN and Al₂O₃ layers is unknown. Our postulate is that the AlN layer has either very high density of intrinsic point defects (e.g silicon and oxygen point

defects) or extended defects like dislocations [31]. The Al₂O₃ layer is expected to contain oxygen related intrinsic defects [32]. These defects are presumably the cause of the current leakage through the AlN and Al₂O₃ layers.

The SiO₂/AlN and SiO₂/Al₂O₃ stack samples have effective breakdown field, if we consider the dual dielectric as a single dielectric, of ~ 8 MV/cm (dashed curve for SiO₂/AlN and dash dotted curve for the SiO₂/Al₂O₃ sample). However, the breakdown electric field across the AlN or Al₂O₃ layer in the stack is ~ 4 MV/cm or ~ 5.5 MV/cm. Addition of SiO₂ on the top of AlN layer does not significantly improve the breakdown properties of the AlN or Al₂O₃ but allows the use of higher gate voltages for device operation.

4. Conclusions

CV analysis at room temperature shows that single crystalline AlN and amorphous Al₂O₃ layer have good interface quality in terms of low density of interface states in n-type 4H-SiC MIS capacitors. A significant electron trapping is observed within the AlN or Al₂O₃ when the MIS capacitors are biased into accumulation resulting in a large flatband voltage shift towards higher gate voltages. This can be connected to the relatively low breakdown field (~ 3 MV/cm or ~ 5 MV/cm) of the AlN or Al₂O₃ layers. It is possible to slightly improve the breakdown field of the MIS devices by depositing a SiO₂ layer on top of the AlN or Al₂O₃. More work is needed in optimizing the growth conditions of the dielectrics and resolving the question of electron trapping within the AlN and Al₂O₃ layers. In summary, the AlN and Al₂O₃ MIS samples show very promising results in terms of interface state densities but electron injection into both layers is currently preventing their practical use.

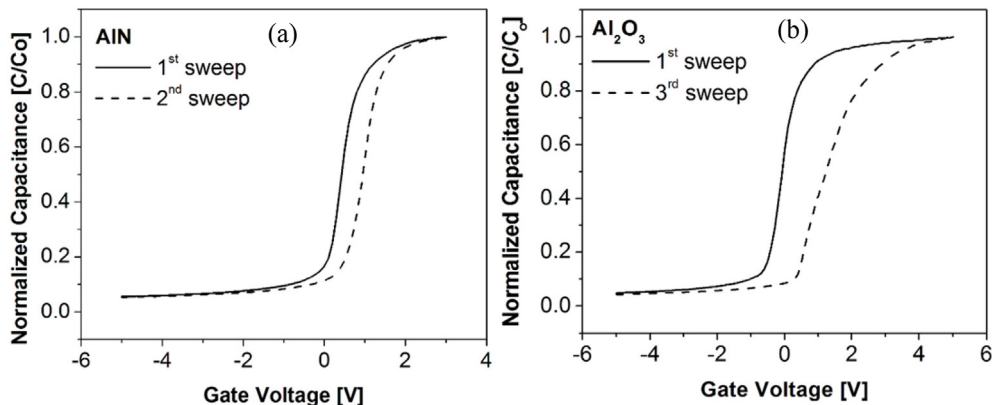


Fig. 3. Subsequent 100 kHz CV sweeps for single layer (a) AlN and (b) Al₂O₃ sample at room temperature.

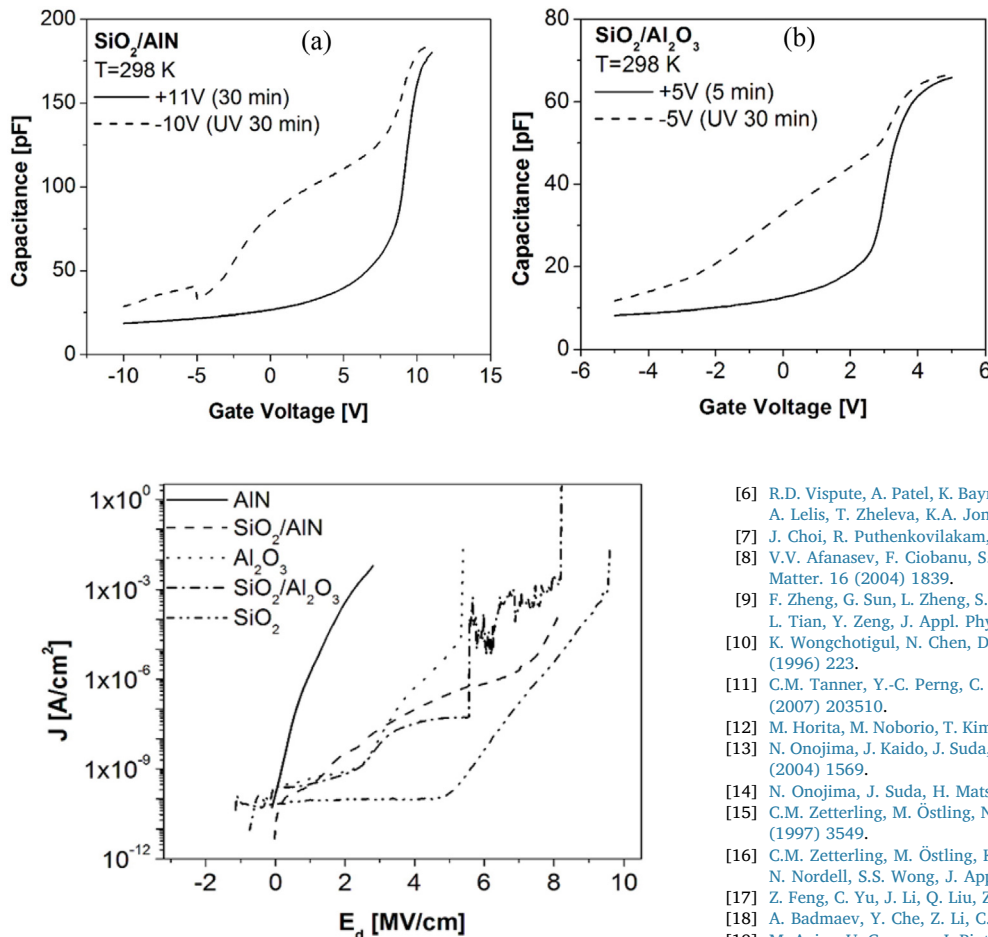


Fig. 5. Comparison of leakage current density versus effective electric field (J - E) for differently prepared MIS samples.

Acknowledgements

This work was financially supported by The Icelandic Research Fund. We also acknowledge support from the Swedish Foundation for Strategic Research (SSF), and the Knut and Alice Wallenberg Foundation (KAW).

References

- [1] Y. Jia, H. Lv, Q. Song, X. Tang, L. Xiao, L. Wang, G. Tang, Y. Zhang, *Appl. Surf. Sci.* 397 (2017) 175.
- [2] S.R. Kodigala, S. Chattopadhyay, S. Overton, I. Ardoin, B.J. Gordon, D. Johnstone, D. Roy, D. Barone, *Appl. Surf. Sci.* 330 (2015) 465.
- [3] T. Kimoto, *Jpn. J. Appl. Phys.* 54 (2015) 040103.
- [4] M. Nawaz, Hindawi Publishing Corporation Active and Passive Electronic Components, (2015), p. 1 (2015).
- [5] M.O. Aboelfotoh, R.S. Kern, S. Tanaka, R.F. Davis, C.I. Harris, *Appl. Phys. Lett.* 69 (1996) 2873.

Fig. 4. Electron injection and emission in and out of traps located within (a) the AlN or (b) Al_2O_3 layer. The black solid 100 kHz CV curves are recorded after which electrons are intentionally injected into the AlN or Al_2O_3 by accumulation bias stress for certain period. The dotted 100 kHz CV curves are recorded after applying negative bias stress with UV illumination to the samples for 30 min.

- [6] R.D. Vispute, A. Patel, K. Baynes, B. Ming, R.P. Sharma, T. Venkatesan, C.J. Scozzie, A. Leles, T. Zheleva, K.A. Jones, *MRS Online Proc. Libr.* 595 (1999) F99W11.3.
- [7] J. Choi, R. Puthenkovilakam, J.P. Chang, *Appl. Phys. Lett.* 86 (2005) 192101.
- [8] V.V. Afanasev, F. Ciobanu, S. Dimitrijevic, G. Pensl, A. Stesmans, *J. Phys. Condens. Matter.* 16 (2004) 1839.
- [9] F. Zheng, G. Sun, L. Zheng, S. Liu, B. Liu, L. Dong, L. Wang, W. Zhao, X. Liu, G. Yan, L. Tian, Y. Zeng, *J. Appl. Phys.* 113 (2013) 044112.
- [10] K. Wongchotigul, N. Chen, D.P. Zhang, X. Tang, M.G. Spencer, *Mater. Lett.* 26 (1996) 223.
- [11] C.M. Tanner, Y.-C. Perng, C. Frewin, S. Sadow, J.P. Chang, *Appl. Phys. Lett.* 91 (2007) 203510.
- [12] M. Horita, M. Noborio, T. Kimoto, J. Suda, *IEEE Trans. Electron Dev.* 35 (2014) 339.
- [13] N. Onojima, J. Kaido, J. Suda, T. Kimoto, H. Matsunami, *Mater. Sci. Forum* 457–460 (2004) 1569.
- [14] N. Onojima, J. Suda, H. Matsunami, *Appl. Phys. Lett.* 80 (2002) 76.
- [15] C.M. Zetterling, M. Östling, N. Nordell, O. Schön, M. Deschler, *Appl. Phys. Lett.* 70 (1997) 3549.
- [16] C.M. Zetterling, M. Östling, K. Wongchotigul, M.G. Spencer, X. Tang, C.I. Harris, N. Nordell, S.S. Wong, *J. Appl. Phys.* 82 (1997) 2990.
- [17] Z. Feng, C. Yu, J. Li, Q. Liu, Z. He, X. Song, J. Wang, S. Cai, *Carbon* 75 (2014) 249.
- [18] A. Badmaev, Y. Che, Z. Li, C. Wang, C. Zhou, *ACS Nano* 6 (2012) 3371.
- [19] M. Avic, U. Grossner, I. Pintilie, B.G. Svensson, M. Servidori, R. Nipoti, O. Nilsen, H. Fjellvag, *J. Appl. Phys.* 102 (2007) 054513.
- [20] S.S. Suvanam, M. Usman, D. Martin, M.G. Yazdi, M. Linnarsson, A. Tempez, M. Götelid, A. Hallén, *Appl. Surf. Sci.* 433 (2018) 108.
- [21] M. Usman, S.S. Suvanam, M.K. Linnarsson, A. Hallén, *Mater. Sci. Semicond. Process.* 81 (2018) 118.
- [22] H. Yoshioka, M. Yamazaki, S. Harada, *AIP Adv.* 6 (2016) 105206.
- [23] T. Hatayama, S. Hino, N. Miura, T. Oomori, E. Tokumitsu, *IEEE Trans. Electron Devices* 55 (2008) 2041.
- [24] J.T. Chen, J.W. Pomeroy, N. Rorsman, C. Xia, C. Virojanadara, U. Forsberg, M. Kuball, E. Janzén, *J. Cryst. Growth* 428 (2015) 54.
- [25] R.Y. Khosa, E.B. Thorsteinsson, M. Winters, N. Rorsman, R. Karhu, J. Hassan, E.Ö. Sveinbjörnsson, *AIP Adv.* 8 (2018) 025304.
- [26] F. Allerstam, G. Gudjonsson, H.Ö. Ólafsson, E.Ö. Sveinbjörnsson, T. Rödle, R. Jos, *Semicond. Sci. Technol.* 22 (2007) 307.
- [27] E.H. Nicollian, J.R. Brews, *MIS (Metal Oxide Semiconductor) Physics and Technology*, John Wiley & Sons, New York, USA, 1982.
- [28] J.A. Cooper Jr., *Phys. Status Solidi* 162 (1997) 305.
- [29] M. Sadeghi, O. Engström, *Microelectron. Eng.* 36 (1997) 183.
- [30] S. Berberich, P. Godignon, M.L. Locatelli, J. Millán, H.L. Hartnagel, *Solid-State Electron.* 42 (1998) 915.
- [31] L. Gordon, J.L. Lyons, A. Janotti, C.G. Van de Walle, *Phys. Rev. B* 89 (2014) 085204.
- [32] L.X. Yu, W.Y. Yu, P.Z. Yang, L.C. Zhan, W. Jia, B. Yun, T.Y. Dan, L.K. An, S.H. Jun, *Chin. Phys. B* 24 (2015) 087304.